Biochimica et Biophysica Acta, 766 (1984) 666–678
Elsevier

BBA 41599

EXCITON INTERACTIONS IN DIMERS OF BACTERIOCHLOROPHYLL AND RELATED MOLECULES

AVIGDOR SCHERZ * and WILLIAM W. PARSON

Department of Biochemistry, University of Washington, Seattle, WA 98195 (U.S.A.)

(Received March 8th, 1983)

Key words: Bacteriochlorophyll; Bacteriopheophytin; Circular dichroism; Absorption spectroscopy; Exciton

Formalisms are developed for calculating the absorption wavelengths, dipole strengths and rotational strengths for dimers of bacteriochlorophyll and related molecules. The expressions explicitly consider the mixing of bacteriochlorophyll's four main excited states (Q_y, Q_x, B_x and B_y) in the ground and excited states of the dimer. This mixing must be considered in order to account for the hyperchromism and nonconservative circular dichroism found experimentally in oligomers of bacteriochlorophyll and bacteriopheophytin. The spectroscopic properties of the eight absorption bands of a bacteriopheophytin dimer are calculated as functions of the geometry of the dimer. The importance of the mixing of nondegenerate excited states, and of the mixing of doubly-excited states into the dimer's ground state, is evaluated by comparisons with calculations in which these phenomena are neglected. Structures for bacteriopheophytin dimers are found for which most of the calculated spectroscopic properties are consistent with the properties seen experimentally. Possible explanations are considered for the remaining discrepancies between the calculated and observed properties.

Introduction

The bacteriochlorophyll (BChl) in photosynthetic bacteria occurs in pigment-protein complexes that typically contain from two to seven BChl molecules bound to a relatively small, hydrophobic protein [1–4]. The spectroscopic properties of the BChl-protein complexes differ markedly from those of monomeric BChl in organic solvents. The long-wavelength (Q_y) absorption band is shifted to lower energies and is sometimes increased considerably in dipole strength. The circular dichroism (CD) bands frequently have very large rotational strengths, and the CD spectrum in the Q_y region is nonconservative. (The rotational strengths of the positive and negative CD bands do not sum to zero.)

In the accompanying paper [5], we show that absorption and CD spectra resembling those found in vivo can be obtained with oligomers of BChl or bacteriopheophytin (BPh) in mixed aqueous solvent systems, or in micelles of the detergent lauryldimethylamine oxide. The oligomer probably needs to be no larger than a dimer, in order to have such spectra [5,6]. Because the spectral effects are seen with BPh as well as with BChl, they clearly do not depend on specific interactions with ligands that bind to the magnesium. (BPh has two hydrogens in place of magnesium.) Instead, they seem likely to result simply from exciton interactions between neighboring molecules in the oligomer. But the spectra cannot be explained

* Present address: Department of Biochemistry, Weizmann Institute, 76100 Rehovot, Israel.

Abbreviations: BChl, bacteriochlorophyll; BPh, bacteriopheophytin; CD, circular dichroism; ORD, optical rotatory dispersion.

0005-2728/84/$03.00 © 1984 Elsevier Science Publishers B.V.

adequately by considering only the interactions between degenerate transitions in the two molecules. For one thing, the 850 nm absorption band of the BPh oligomer in lauryldimethylamine oxide micelles has a dipole strength that is about 1.7-times greater than the total dipole strength in the Q_y transitions of the monomeric PBh that has formed the aggregate [5]. The summed dipole strengths of the exciton bands that result from interactions between degenerate excited states should be equal to the sum of the dipole strengths of the individual molecules [7,8]. Exciton interactions between degenerate states also are not sufficient to account for the nonconservative CD spectrum of the oligomers. The sum of the rotational strengths of the exciton bands that result from such interactions must be zero [7,8]. Finally, if one considers only degenerate states, a large bathochromic shift of the Q_y absorption band (a shift to longer wavelengths) requires that the Q_y transition dipoles be oriented more or less in parallel. This orientation would give the corresponding CD band a smaller rotational strength than is observed [9].

The large dipole strength and rotational strength of the Q_y band in the oligomers appear to arise at the expense of the higher-energy (Soret and Q_x) bands [5]. Intensity borrowing of this sort, termed hyperchromisim, can be rationalized by considering exciton interactions between nondegenerate states in neighbouring molecules, in addition to interactions between degenerate states. The theory of hyperchromism, which was developed orginally by Tinoco [7,8], has been aplied extensively to nucleic acids and proteins, and recently has been used for anthracene [10]. We here elaborate the theory in a form that is useful for chlorophylls and related molecules, and calculate the spectral properties of dimers with a range of geometries.

Theory

Consider a dimer of BChl or PBh. Each of the monomeric components of the dimer has four main excited states, designated Q_y, Q_x, B_x and B_y, or 1, 2, 3 and 4, in order of increasing energy [11–14]. Zero-order wavefunctions for the ground state and excited state J of a dimer of identical non-overlapping, uncharged and nonpolar molecules (a and b) are:

$$\Psi_G^0 = \phi_{a0}\phi_{b0} \tag{1}$$

$$\Psi_J^0 = \left\{ \phi_{aj}\phi_{b0} - (-1)^J \phi_{a0}\phi_{bj} \right\} 2^{-1/2} \tag{2}$$

where ϕ_{m0} is the wavefunction for the ground state of isolated monomer m, and ϕ_{mj} is that for the monomer's excited state j. The dimer has two exciton states corresponding to the monomer's state j; we designate these by even and odd values of the index J, letting $J = 2j$ or $2j - 1$ with $j = 1$, 2, 3 and 4.

The zero-order energies of the dimer's states are:

$$E_G^0 = 2E_g \tag{3}$$

$$E_J^0 = E_g + E_j - (-1)^J V_{aj,bj} \tag{4}$$

where E_g and E_j are the energies of the gound and excited states of the isolated molecules and $V_{aj,bj}$ is the interaction energy between the two molecules. Because monomeric BChl or PBh probably has only a relatively small permanent dipole moment when the molecule is in the ground state or any of the relevant excited states [13,14], the interaction energies depend mainly on the transition dipole moments. In the point-dipole approximation:

$$V_{aj,bk} = \frac{\boldsymbol{\mu}_{aj} \cdot \boldsymbol{\mu}_{bk}}{|\boldsymbol{R}_{ab}|^3} - \frac{3(\boldsymbol{\mu}_{aj} \cdot \boldsymbol{R}_{ab})(\boldsymbol{\mu}_{bk} \cdot \boldsymbol{R}_{ab})}{|\boldsymbol{R}_{ab}|^5} \tag{5}$$

where $\boldsymbol{\mu}_{mj}$ is the electric transition dipole for the transition $\phi_{m0} \rightarrow \phi_{mj}$, and $\boldsymbol{R}_{ab}$ is the vector connecting the centers of molecules a and b [8]. (The transition dipole $\boldsymbol{\mu}_{mj}$ is $\langle \phi_{mj} | \mu_m | \phi_{m0} \rangle$, where μ_m is the electric dipole operator operating on molecule m.) More accurate results could be obtained by a point-monopole treatment [13,15].

In order to account for hyperchromism, it is necessary to mix other excited states in with Ψ_G^0 and Ψ_J^0. In the absence of permanent dipole moments or other perturbations, Ψ_G^0 mixes only with states in which molecules a and b are both excited [8,16]. Taking a linear combination of the zero-order ground state with these doubly-excited molecular states gives the first-order ground-state

wavefunction:

$$\Psi_G = \left(\phi_{a0}\phi_{b0} + \sum_{j=1}^{4} \sum_{k=1}^{4} g_{jk}\phi_{aj}\phi_{bk} \right) F_G \qquad (6)$$

where $F_G = (1 + \sum_j \sum_k g_{jk}^2)^{-1/2}$. The coefficients g_{jk} are found by first-order perturbation theory to be:

$$g_{jk} = -V_{aj,bk}/h(\nu_{aj} + \nu_{bk}) \qquad (7)$$

where ν_{aj} and ν_{bk} are the frequencies of the optical absorptions associated with excitation of molecules a and b into states j and k, respectively [8]. The factor F_G is needed to normalize Ψ_G, but F_G typically differs from 1.0 by less than two percent.

The doubly-excited molecular states are far enough removed from Ψ_G^0 in energy so that they do not alter the energy of the ground state significantly. However, they can contribute to both the dipole strengths and the rotational strengths of the transitions in the dimer.

The eight excited states of a BChl or BPh dimer can be expressed similarly as linear combinations of the singly-excited molecular states. In some cases, the dominant contributions to a given excited state, Ψ_J, will still come from a particular pair of degenerate molecular states, $\phi_{aj}\ \phi_{b0}$ and $\phi_{a0}\ \phi_{bJ}$. Separating out these contributions and using first-order perturbation theory again, one obtains the approximate expression:

$$\Psi_J \approx \left\{ \phi_{aj}\phi_{b0} - \sum_{k \neq j}^{4} \frac{V_{aj,bk}}{h(\nu_{bk} - \nu_{aj})} \phi_{a0}\phi_{bk} \right\} F_J$$

$$-(-1)^J \left\{ \phi_{a0}\phi_{bj} - \sum_{k \neq j}^{4} \frac{V_{ak,bj}}{h(\nu_{ak} - \nu_{bj})} \phi_{ak}\phi_{b0} \right\} F_J \qquad (8)$$

where:

$$F_J = \left\{ 2 + \sum_{k \neq j}^{4} \left[\frac{V_{aj,bk}}{h(\nu_{bk} - \nu_{aj})} \right]^2 + \sum_{k \neq j}^{4} \left[\frac{V_{ak,bj}}{h(\nu_{ak} - \nu_{bj})} \right]^2 \right\}^{-1/2}$$

Eqn. 8 is essentially equivalent to Tinoco's equation [8] (IIIB-15), but emphasizes the importance of F_J, which can be significantly less than $1/\sqrt{2}$. For simplicity, we have again assumed that the permanent dipole moments of the ground and excited states are negligible compared to the transition dipoles.

Eqn. 8 is useful for analyzing the dimer transitions that arise predominantly from the Q_y or Q_x transitions, because these transitions are relatively well separated in energy from each other and from the B_y and B_x transitions. As long as the interaction energies between the degenerate states are much smaller than the energy gaps between the monomer's transitions, Eqn. 4 also continues to describe the energies of the dimer's states reasonably well. However, Eqns. 4 and 8 are inadequate when one considers the dimer transitions that arise mainly from the B_y or B_x transitions. These transitions are relatively close together in energy, and their interaction energies can be comparatively large because of the large dipole strength of the B_y transition.

For a more general solution, one must use the full secular equation to obtain better descriptions of the dimer's eigenstates. Let the first-order wavefunction of the Jth excited state of the dimer be:

$$\Psi_J = \sum_{q=1}^{8} C_{q,J}\phi_q \qquad (9)$$

where the basis set of wavefunctions ψ_q are $\psi_1 = \phi_{a1}\phi_{b0}$, $\psi_2 = \phi_{a0}\ \phi_{b1}$, $\psi_3 = \phi_{a3}\ \phi_{b0}$, ... and $\psi_8 = \phi_{a0}\ \phi_{b4}$. For consistency of notation, let $\nu_1 = \nu_{a1}$, $\nu_2 = \nu_{b1}$, $\nu_3 = \nu_{a2}$, etc.; and let μ_q be the electric transition dipole for the molecular transition $\phi_{a0}\ \phi_{b0} \rightarrow \psi_q$. We continue to assume that orbital overlap between the two molecules is negligible, and that the doubly-excited states do not affect significantly the energy of the dimer's ground state. This allows one to refer the energies of the dimer's excited states (E_J) to the energy of the zero-order ground state (E_G^0). The transition energies ($\Delta E_J = E_J - E_G^0$) and coefficients ($C_{q,J}$) are obtained as the eigenvalues and eigenvectors of the secular equation $[H_{p,q} - \delta_{p,q}\Delta E_J][C_{q,J}] = 0$, where the elements ($H_{p,q}$) of the Hamiltonian matrix **H** are:

$$\begin{array}{c} \\ \langle\psi_1| \\ \langle\psi_2| \\ \langle\psi_3| \\ \langle\psi_4| \\ \vdots \\ \langle\psi_3| \end{array} \begin{array}{c} \begin{array}{cccccc} |\psi_1\rangle & |\psi_2\rangle & |\psi_3\rangle & |\psi_4\rangle & \cdots & |\psi_8\rangle \end{array} \\ \begin{bmatrix} h\nu_1 & V_{a1,b1} & 0 & V_{a1,b2} & \cdots & V_{a1,b4} \\ V_{a1,b1} & h\nu_2 & V_{a2,b1} & 0 & \cdots & 0 \\ 0 & V_{a2,b1} & h\nu_3 & V_{a2,b2} & \cdots & V_{a2,b4} \\ V_{a1,b2} & 0 & V_{a2,b2} & h\nu_4 & \cdots & 0 \\ \vdots & \vdots & \vdots & \vdots & \ddots & \vdots \\ V_{a1,b4} & 0 & V_{a2,b4} & 0 & \cdots & h\nu_8 \end{bmatrix} \end{array}$$

Zero elements indicate that the elementary, singly-excited states of an individual molecule are not mixed if the other molecule remains in its ground state. These states could be mixed by the perturbation due to a permanent dipole in the neighboring molecule, but as stated above, permanent diples have been neglected.

We have used a program written in BASIC for a minicomputer to solve for the coefficients and energy associated with each excited state of a dimer. The interaction energies ($V_{aj,bk}$) are first obtained for a specified geometry using Eqn. 5. The Hamiltonian then is diagonalized by Jacobi's method, essentially as described by Carnahan et al. [17]. This procedure generates an 8×8-matrix of coefficients, which are automatically scaled so as to normalize the wavefunctions. The algorithm generally converges within two or three iterations.

To calculate the electric and magnetic transition dipoles of the dimer, it is useful to arrange the normalized ground-state coefficients, $g_{jk}\ F_G$ (Eqns. 6 and 7), in a matrix, **G**, with the same dimensions and structure as the Hamiltonian matrix. The element $G_{p,q}$ ($p,q = 1\ldots, 8$) then represents the contribution to the ground state from the doubly-excited dimer containing the two singly-excited elementary states whose transition dipolar interaction is expressed by $H_{p,q}$. The terms on the main diagonal are set to zero to avoid indicating double excitation of the same monomer; other elements of the Hamiltonian that would indicate this are already zero. **G** is thus:

$$\begin{pmatrix} 0 & g_{11} & 0 & g_{12} & \cdots & g_{14} \\ g_{11} & 0 & g_{21} & 0 & \ldots & 0 \\ 0 & g_{21} & 0 & g_{22} & \cdots & g_{24} \\ g_{12} & 0 & g_{22} & 0 & \ldots & 0 \\ \vdots & \vdots & \vdots & \vdots & \ddots & \vdots \\ g_{14} & 0 & g_{24} & 0 & \ldots & 0 \end{pmatrix} F_G$$

The electric transition dipole for the transition $\Psi_G \xrightarrow{h\nu} \Psi_J$ is:

$$\boldsymbol{\mu}_J = \langle \Psi_J | \underset{\sim}{\mu}_a + \underset{\sim}{\mu}_b | \Psi_G \rangle \tag{12}$$

Combining Eqns. 6, 9, 11 and 12, and evaluating the integrals gives:

$$\boldsymbol{\mu}_J = \sum_{q=1}^{8} \left(C_{q,J} + \sum_{p=1}^{8} C_{p,J} G_{p,q} \right) \boldsymbol{\mu}_q \tag{13}$$

The terms $C_{q,J}\boldsymbol{\mu}_q$ represent upward transitions from the main component of the dimer's ground state ($\phi_{a0}\phi_{b0}$) to the various molecular excited states (ψ_q) that make up the excited state Ψ_J of the dimer. The terms $\sum_{p=1}^{8} C_{p,J} G_{p,q} \boldsymbol{\mu}_q$ represent downward transitions from one of the doubly-excited elementary states that are present in the dimer's ground state to one of the singly-excited molecular states.

The transition dipole $\boldsymbol{\mu}_J$ can be calculated immediately by vector addition using Eqn. 13, once all of the coefficients for the ground and excited states are known. The corresponding dipole strength is $|\boldsymbol{\mu}_J|^2$.

The rotational strengths of the dimer's absorption bands are given by:

$$\mathscr{R}_J = \mathrm{Im}(-\boldsymbol{m}_J \cdot \boldsymbol{\mu}_J) = \{\mathrm{Im}(-\boldsymbol{m}_J)\} \cdot \boldsymbol{\mu}_J \tag{14}$$

where $\boldsymbol{m}_J$ is the magnetic transition dipole of the transition $\Psi_G \rightarrow \Psi_J$, and Im means the imaginary part of the function within the parentheses 4 [8]. We assume that the absorption bands of the individual monomers have negligibly small magnetic transition dipoles, compared to the magnetic dipoles that result from exciton interactions. This is consistent with (but not proved by) the observation that the CD spectra of monomeric BChl and BPh are very weak relative to the CD spectra of the aggregated species. It is consistent also with the fact that optical transitions are strongly allowed electrically. Strong electric and magnetic dipole transitions are mutually exclusive in molecules that are approximately centrosymmetric, because of their different symmetry transformations [15,18].

For a transition such as $\phi_{a0} \rightarrow \phi_{aj}$ in an individual molecule, the magnetic transition dipole $\boldsymbol{m}_{aj}$ can be expressed as:

$$\boldsymbol{m}_{aj} = -\frac{\pi \mathrm{i}}{c} \nu_{aj} \boldsymbol{R} \times \boldsymbol{\mu}_{aj}$$

where the position vector $\boldsymbol{R}$ points to the center of electron density on the molecule and $c = 3 \cdot 10^{10}$ cm $\cdot$ s^{-1} [8]. Using Eqn. 13, the magnetic transition dipoles of the dimer can be written:

$$\boldsymbol{m}_J = -\frac{\pi \mathrm{i}}{c} \sum_{q=1}^{8} \nu_q \left[C_{q,J} - \sum_{p=1}^{8} C_{p,J} G_{p,q} \right] \boldsymbol{R}_q \times \boldsymbol{\mu}_q \tag{15}$$

$\boldsymbol{R}_q$ points to the monomer (a or b) on which transition dipole μ_q is located. The negative sign before the sum over p results from the fact that these terms reflect downward molecular transitions, as was noted above in connection with Eqn. 13; $\boldsymbol{m}_{aj}$ differs from μ_{aj} in depending on the direction of the transition.

The calculation of $\mathscr{R}_J$ is simplified by placing molecule a at the origin of the coordinate system. $|\boldsymbol{R}_q|$ then is zero for q odd, and Eqn. 15 reduces to:

$$\mathrm{Im}[-\boldsymbol{m}_J] = \frac{\pi}{c}\boldsymbol{R}_b \times \sum_{j=1}^{4} \nu_q \left(C_{q,J} - \sum_{p=1}^{8} C_{p,J} G_{p,q} \right) \mu_q \qquad (16)$$

with:

$q = 2j$

The vector sum over j is the same as the sum over q in Eqn. 13, exept that only even values of q are included, each term is weighted by ν_q, and the sign of the nested sum over p is negative. $\mathscr{R}_J$ can be calculated straightforwardly from Eqns. 13, 14 and 16.

To test the reliability of the coefficients $C_{q,J}$ and $G_{p,q}$, it is useful to calculate the quantity $\Delta\mathscr{R} = \sum_{J=1}^{8} \mathscr{R}_J / (\sum_{J=1}^{8} \mathscr{R}_J^2)^{1/2}$, which is principle should be zero. In the calculations summarized below, $\Delta\mathscr{R}$ was generally 10^{-3} or smaller. When the mixing of the doubly-excited states with the ground state was omitted, $\Delta\mathscr{R}$ was generally less than 10^{-6}. This indicates that the diagonalization of **H** to find the coefficients $C_{q,J}$ for the singly-excited states is numerically accurate, as it should be if the convergence criterion in the Jacobi algorithm is sufficiently stringent. (We used the criterion $1 - S1/S2 < 10^{-7}$, where $S1$ and $S2$ are the sums of the squares of the diagonal elements of **H** before and after a given iteration of the Jacobi procedure.) The coefficients $G_{p,q}$ for the ground state are less accurate, because they are obtained by first-order perturbation theory (Eqn. 7), rather than by diagonalizing the 17×17-Hamiltonian of the doubly-excited states and the zero-order ground state. However, the increased accuracy that could be obtained by full diagonalization is small relative to the other approximations inherent in the Hamiltonians.

Application to bacteriopheophytin dimers

To calculate the dipole strengths and rotational strengths for a BPh or BChl dimer, one first must know the magnitudes and directions of the molecular transition dipoles μ_{aj} and μ_{bk}. Fig. 1 defines the angles that we have used to specify the orientations of the dipoles. Molecule a is centered at the origin of a right-handed Cartesian coordinate system. Its Q_x and Q_y transition dipoles are taken to be orthogonal [11–14], and are used to define the x and y axes. The B_x transition dipole is assumed to be parallel to Q_x, and the B_y dipole to Q_y. Vector $\boldsymbol{R}_b$ (x, y, z) (not shown in the figure) locates the center of molecule b. Direction angles α_y, β_y and γ_y specify the orientations of the Q_y and B_y transition dipoles of molecule b with respect to the x, y and z axes; angles α_x, β_x and γ_x give the orientations of the Q_x and B_x transition dipoles. Five of these six angles are independent.

The squared magnitudes of the transition dipoles, the dipole strengths, are obtained by integrating over the absorption bands of the mono-

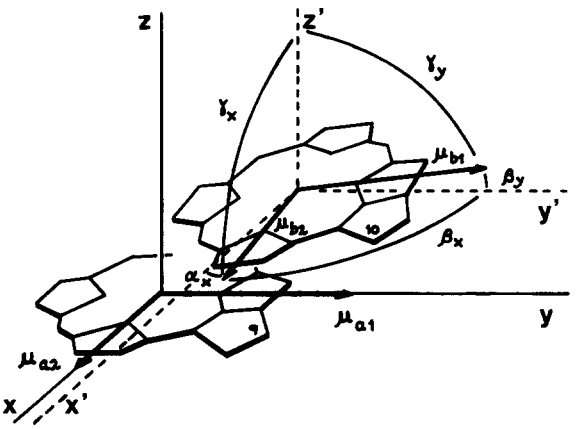

Fig. 1. Angles used to specify the geometry of BPh dimers. Transition dipoles μ_{a2} (Q_x) and μ_{a1} (Q_y) of molecule a define the x- and y-axes of a right-handed Cartesian coordinate system with the center of molecule a at the origin. Axes x', y' and z' are parallel to x, y, and z. Direction angles α_y, β_y and γ_y define the orientations of transition dipole μ_{b1} (Q_y) of molecule b, relative to the x, y, and z axes. Angles α_x, β_x, and γ_x define the orientations of μ_{b2} (Q_x). (α_y is not indicated in the figure.) Carbons 10 of molecule b and 9 of molecule a are labeled. The carbomethoxy group on C10 projects below the plane of the ring.

meric pigments:

$$|\mu_{mj}|^2 = 9.18 \cdot 10^{-3}\left[9n/(n^2+2)^2\right] \int(\varepsilon_{mj}/\nu)\mathrm{d}\nu \text{ debye}^2$$

where n is the refractive index and ε_{mj} (ν) is the molar extinction coefficient for transition j of molecule m [19]. But there is an immediate problem connected with the shapes of the absorption bands, The Q_x and Q_y bands of monomeric BChl and BPh have distinct vibrational shoulders that lie about 1300 and 2800 cm^{-1} above the principal band (Fig. 2). Whether or not the higher vibrational levels should be included in the integral depends on the strength of the interaction between the two molecules. In the limit of strong coupling, when $2V_{aj,bk}$ is much greater than the separation between the higher vibrational levels and the (0,0) level, the integration should include the higher levels [20]. The result of the interaction in this limit is that the entire absorption band is incorporated into the exciton bands, which are sharpened and shifted strongly in energy relative to the original band. As Fig. 2 illustrates, this situation appears to apply to the interactions between Q_y transitions in the oligomers of BChl and BPh whose preparation is described in the accompanying paper [5]. In the opposite limit of very weak coupling, the various vibrational states of the two molecules can be viewed as interacting independently. The exciton bands resulting from interaction of the main vibrational bands experience the greatest shift of wavelength, because their dipole strength is greatest. The weak-coupling limit appears to apply to the Q_x band of the BChl and BPh oligomers. In this case, the main exciton band is shifted slightly to the blue and experiences hypochromism relative to the original band, whereas the higher vibrational bands hardly change (Fig. 2). To calculate the relevant transition dipole for the Q_x band, it therefore seems appropriate to take the integral only over the main vibronic band.

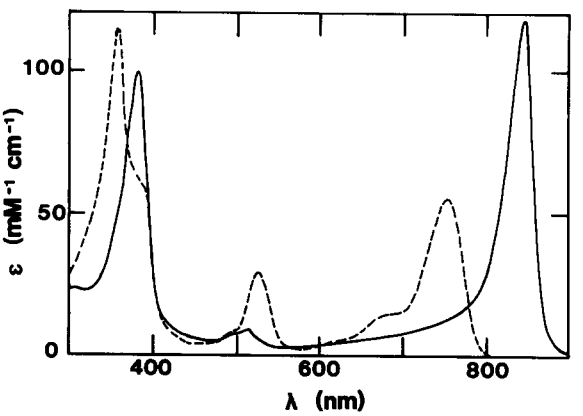

Fig. 2. Absorption spectra of monomeric BPh in acetic acid (— — —), and of oligomeric BPh in acetic acid-water mixtures or in LIDAO micelles (———). Redrawn from Figs. 1 and 4 of Ref. 5, with estimated corrections for the monomeric BPh remaining in the samples of oligomers. The extinction coefficients are expressed on the basis of the molarity of monomeric BPh.

Evaluation of the B_x and B_y transition dipoles for BChl and BPh presents additional problems. These transitions overlap in the absorption spectra of the monomeric pigments, and resolution of the components is uncertain because the band shapes are not known. The B_y transition actually may consist of several overlapping y-polarized transitions [14]. It would be helpful to have the linear dichroism spectra of well-oriented monomeric pigments, but these have not been measured to our knowledge. For simplicity, we assumed that the bands are Gaussian, and used the entire bands to estimate the dipole strengths.

Absorption maxima and dipole strengths (in debye^2) calculated in this way for monomeric BPh are: Q_y (758 nm), 39; Q_x (528 nm), 13; B_x (375 nm), 37; and B_y (355 nm), 80. These are indicated with dashed lines in fig. 3A. We used the same set of transition dipoles to calculate the interaction energies between both degenerate and nondegenerate transitions.

This treatment of the absorption band shapes is clearly an oversimplification. The coupling of vibrational and electronic transitions can affect the absorption and CD spectra of an oligomer strongly, even in cases when the vibronic bands are not separated as widely as they are in BPh. More rigorous treatments of vibronic coupling in exciton interactions have been developed recently [21–24], and one of these has been applied to BChl-protein complexes [25]. However, these treatments consider only a single excited electronic state in each of the interacting molecules. Extending them to include four excited states is not straightforward. Although probably not highly ac-

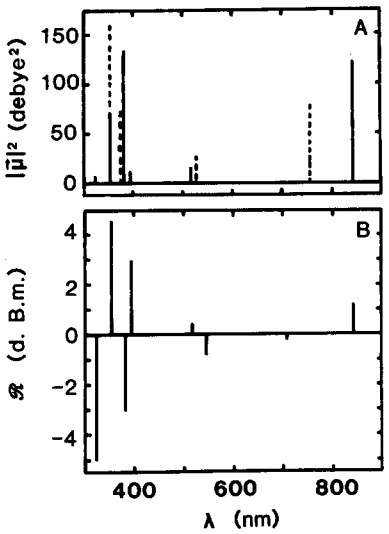

Fig. 3. (A) (— — —), dipole strengths for monomeric BPh, calculated from the data of Fig. 2 as explained in the text. The dipole strengths have been multiplied by 2 to facilitate comparisons with those calculated for BPh dimers. (———), dipole strengths calculated for a BPh dimer with the following structural parameters: $\boldsymbol{R}_b$ $(x, y, z) = (0.5, 3.5, 3.6)$ Å, $\alpha_y = 79°$, $\beta_y = 15°$, $\gamma_y = 80°$, $\alpha_x = 16.36°$, $\beta_x = 102.8°$, $\gamma_x = 80°$. Interactions between both degenerate and nondegenerate excited states were included in the calculations. Perturbation of the ground state by doubly excited states also was included. Identical results are obtained if the directions of the Q_x (and B_x) or Q_y (and B_y) transition dipoles of molecule *b* are changed by 180°. (B) Rotational strengths calculated for the same dimer. The units are debye Bohr magnetons (d.B.m.); 1 d.B.m. = $9.2 \cdot 10^{-39}$ esu²·cm².

curate, the simple treatment of the band shapes used here should be helpful for considering the major effects of interactions with additional excited states.

The solid lines in Fig. 3A show the absorption wavelengths and dipole strengths calculated for a BPh dimer with a structure similar to that sketched in Fig. 2. For simplicity, the two molecules are assumed to be indentical, although the theory developed above does not require this assumption. Molecule *b* is displaced from *a* by $\boldsymbol{R}_b = (-0.5, 3.5, 3.6)$ Å, which gives a center-to-center distance of 5.05 Å. The bacteriochlorin ring of molecule *b* is tilted so that its Q_y transition dipole makes an angle (γ_y) of 80° with respect to the *z* axis. The Q_x transition dipole makes an angle (γ_x) of 80° with respect to this axis. The angle between the Q_y transition dipoles of the two molecules (β_y) is 15°. Angle α_y (79°) is determined by β_y and γ_y, and a choice of sign ($\cos \alpha_y > 1$) that specifies the direction of rotation of molecule *b* about the *z*-axis. Angle α_x (16.4°) is determined by another choice of sign ($\cos \alpha_x > 0$). Angle β_x (102.8°) is determined uniquely by the previous choices. The calculations (Fig. 3A) agree qualitatively with the observed spectrum of the BPh oligomer in lauryldimethylamine oxide vesicles (Fig. 2). The main Q_y transition is predicted to be red-shifted to 843 nm, and to exhibit string hyperchromism. The short-wavelength Q_y transition at 707 nm has a dipole strength of only 0.45 debye², too small to show in the figure. The calculations also predict the hypochromism and hypsochromic shift that are seen in the Q_x region, and the net hypochromism and bathochromic shift seen in the Soret region.

As shown in Fig. 3B, the calculated CD spectrum in the Q_y region is strongly nonconservative. The long-wavelength Q_y transition at 843 nm has a positive rotational strength that is 5.9-times greater than the negative rotational strength of the short-wavelength transition at 707 nm. This asymmetry is balanced by net negative rotational strengths in the Q_x and Soret regions. These features agree qualitatively with the observed CD spectrum [5]. However, the observed spectrum has a broad negative band near 815 nm that is not predicted by the theory, and the weak negative band calculated to occur near 707 nm is not seen experimentally. We return to these points below.

The spectroscopic properties shown in Fig. 3 are unaffected if molecule *b* is rotated by 180° about its Q_x or Q_y transition dipole. (A 180° rotation about the Q_x transition dipole, μ_{b2} converts the direction angles for Q_y into $\alpha_y = 101°$, $\beta_y = 165°$ and $\gamma_y = 100°$; a 180° rotation about μ_{b1} converts the direction angles for Q_x into $\alpha_x = 163.6°$, $\beta_x = 77.2°$ and $\gamma_x = 100°$.) Such rotations affect the signs, but not the magnitudes of the coefficients $C_{p,J}$; they leave the transition wavelengths, dipole strengths and rotational strengths the same. We therefore cannot distinguish between the dimer illustrated in Fig. 1 and the three chemicallly different structures that could be obtained by inverting molecule *b*. The ground states of these structures presumably do differ in energy,

however. The structure that is illustrated might allow the C10a ester carbonyl of molecule *b* to interact with the C9 keto group of molecule a through a hydrogen-bonded H_2O [5].

Figs. 4–8 show the relative contributions of degenerate and nondegenerate interactions to the calculated spectroscopic properties, and also show how the geometry of the dimer affects the results. For Figs. 4 and 5, $\boldsymbol{R}_b$, γ_x and γ_y were held constant at the values used in Fig. 3. Angle β_y was varied about its minimum value of 10° (90° − γ_y). Values of β_y on the left-hand side of 10° in each panel represent right-handed rotations of molecule *b* about the *z*-axis (cos $\alpha_y < 0$). Those on the right of 10° represent left-handed rotations (cos $\alpha_y > 0$).

The dashed curves in Figs. 4 and 5 show the spectroscopic properties that are calculated if one considers interactions between degenerate singly-excited states only. Off-diagonal terms of **H** were dropped for these calculations, except for terms (such as $H_{1,2}$) that represent degenerate interactions. The perturbation of the ground state also was neglected. The numbers by the curves give the index *J* that identifies the corresponding excited state of the dimer. Odd and even values of *J* represent symmetric and antisymmetric combinations of the dominant molecular excited states, as explained above in connection with Eqn. 2. The solid curves in Figs. 4 and 5 show the results of calculations including nondegenerate interactions

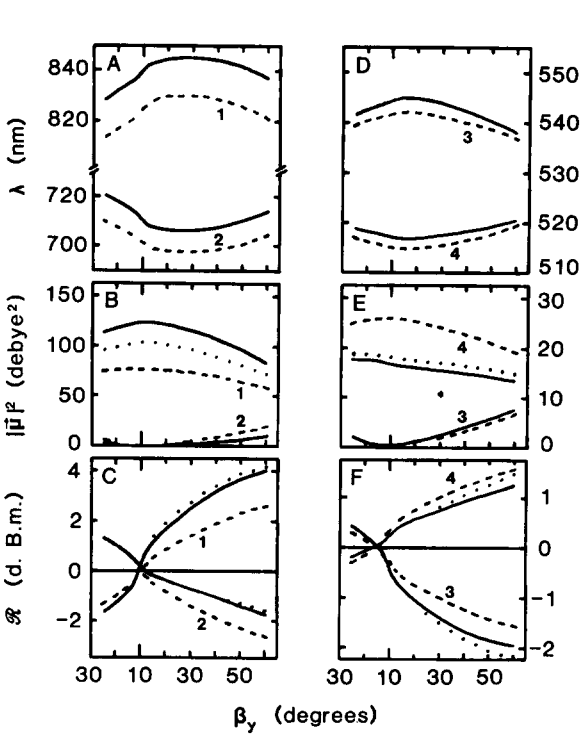

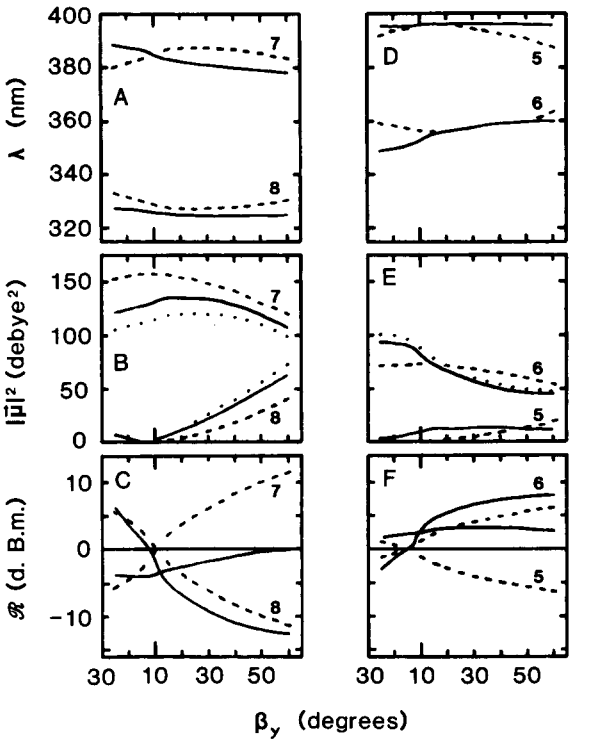

Fig. 4. Absorption wavelengths (panels A and D), dipole strengths (B and E), and rotational strengths (C and F) calculated for the first four absorption bands of a BPh dimer, as a function of angle β_y. Fixed structural parameters: $\boldsymbol{R}_b = (0.5, 3.5, 3.6)$ Å, $\gamma_x = 100°$ and $\gamma_y = 80°$. The normal to the bacteriochlorin ring of molecule *b* makes a constant angle of 14.22° with the *z'* axis, and describes a cone about this axis as β_y is varied. For the structures represented by values of β_y on the left-hand side of 10° in each panel, α_y is chosen so that cos $\alpha_y < 0$. For those with β_y on the right of 10°, cos $\alpha_y > 0$. In all cases, cos $\alpha_x > 0$. Dashed curves: only degenerate interactions considered; no perturbation of ground state. Dotted curves: both degenerate and nondegenerate interactions considered in the excited states; no perturbation of ground state. Solid curves: both degenerate and non-degenerate interactions considered in excited states; perturbation of ground state included. Numbers 1–4 by curves are asignments of transitions using index *J*, as explained in text.

Fig. 5. Absorption wavelengths (panel A and D), dipole strengths (B and E), and rotational strengths (C and F) calculated for transitions 5–8 of a BPh dimer, as a function of β_y. Structural parameters and other conventions as in Fig. 4.

and including the pertubation of the ground state.

For the range of geometries illustrated, the degenerate interactions give a substantial splitting of the Q_y and B_y transitions (dashed curves 1 and 2 in Fig. 4A, and 7 and 8 in Fig. 5A). The splitting is maximal when β_y is approx. 25°C. Most of the dipole strength of the Q_y or B_y transition goes into the longer-wavelength band (curves 1 and 7 in Figs. 4B and 5B). The sum of the dipole strengths in each pair of exciton bands is equal to that of the isolated molecular transitions. In the Q_x and B_x transitions, the exciton splitting is smaller (Figs. 4D and 5D), and the dipole strength goes mainly to the band that shifts to shorter wavelengths (Figs. 4E and 5E). In all cases, the rotational strengths of the two exciton bands are equal in magnitude and opposite in sign (Figs. 4C, 4F, 5C and 5F).

When nondegenerate interactions are included, transitions 1–4 all move to longer wavelengths (solid curves in Fig. 4A and D). This increases the bathochromic shift of the main Q_y band, and decreases the shift of the Q_x band to shorter wavelengths. The dipole strength of the main Q_y band increases substantially, and that of the main Q_x band decreases (Fig. 4B and E). The rotational strengths of the two exciton bands in each pair become unequal in magnitude. For the geometries represented on the right-hand sides of Fig. 4C and F, including the nondegenerate interactions makes the rotational strength of the long-wavelength Q_y transition increasingly positive, and that of the short-wavelength Q_y transition less negative. The rotational strength of the short-wavelength transition goes through zero at β_y approx 12°, when the long-wavelength transition still has a rotational strength of approx. +0.7. The nondegenerate interactions have an opposite effect on the rotational strengths of the Q_x transitions. The net rotational strength of these transitions is negative for the geometries on the right-hand sides of Figs. 4C and F.

The effects of the nondegenerate interactions on the Soret transitions are more complicated, because the molecular B_x and B_y states are extensively mixed in the dimer and the nature of the mixture varies strongly with the geometry. For the geometries illustrated, the nondegenerate interactions affect the rotational strengths of transitions 5 and 7 particularly radically (Figs. 5C and F). The dipole strength of transition 7 is decreased, accounting for much of the increase in the dipole strength of the Q_y transition.

The dotted curves in Fig. 4 and 5 show the results of calculations in which the perturbation of the ground state by the doubly excited states was neglected. Nondegenerate interactions of the singly excited states were still considered. The perturbation of the ground state has substantial effects on the dipole strengths of transitions 1 and 7 (Figs. 4B and 5B); the effects on the dipole strengths of the other transitions are smaller. The calculated asymmetry of the Q_y rotational strengths is increased slightly if one neglects the ground state (Fig. 4C).

Fig. 6 shows the effects of changing angle γ_x. Angles α_y, β_y and γ_y and $\boldsymbol{R}_b$ are held constant at the values used for Fig. 3. Angles α_x and β_x vary with γ_x, but are chosen so that $\cos \alpha_x > 0$. Changing γ_x between 75° and 105° has relatively small effects on the calculated wavelengths or dipole strengths of the dimer's transitions, but it alters the rotational strengths strongly. As γ_x is decreased below 90°, the rotational strength of the long-wavelength Q_y band (transition 1) becomes increasingly positive, and that of the short-wavelength Q_y band (transition 2) becomes less nega-

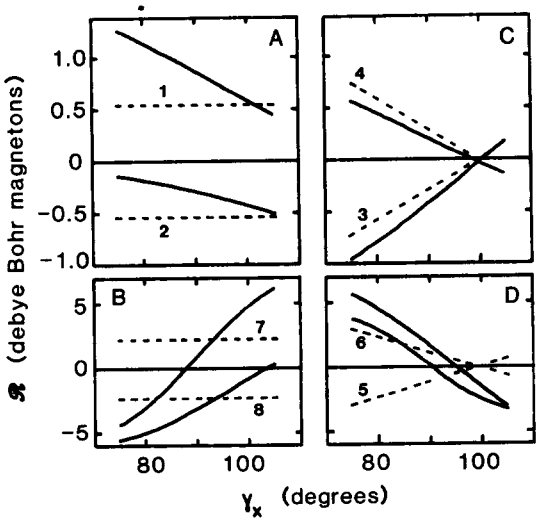

Fig. 6. Rotational strengths calculated for transitions 1–8 of a BPh dimer, as a function of γ_x. Fixed parameters: $\boldsymbol{R}_b$ = (0.5, 3.5, 3.6) Å, $\alpha_y = 79°$, $\beta_y = 15°$, $\gamma_y = 80°$, $\cos \alpha_x > 0$. Dashed and solid curves as in Fig. 4.

tive. The rotational strengths of two of the Soret transitions become more negative (Fig. 6B); those of the other two, more positive (Fig. 6D). These effects depend heavily on nondegenerate interactions. If one considers only the degenerate interactions, the rotational strengths of transitions 1, 2, 7 and 8 are independent of γ_x (dashed curves in Figs. 6A and B).

Changing angle γ_y has comparable effects on the rotational strengths, and also alters the transition wavelengths and dipole strengths. This is difficult to illustrate, because the results depend critically on the value of β_y. In general, the bathochromic shift, hyperchromism, and positive rotational strength of the long-wavelength Q_y transition can all be made greater than shown in Fig. 3 by decreasing γ_y toward 75° and increasing β_y. However, values of γ_x and γ_y that differ from 90° by more than about 10° may not be physically meaningful unless the z-component of $\boldsymbol{R}_b$ is increased, because the two molecules would overlap.

Fig. 7 illustrates the effects of changing the center-to-center distance between the two molecules, $|\boldsymbol{R}_b|$. For these calculations, all of the angles specifying the orientations of $\boldsymbol{R}_b$ and the molecular transition dipoles were held constant in the geometry used for Fig. 3. No attempt was made to correct for the distance dependence of the dielectric constant. The figure shows the calculated wavelengths, dipole strengths and rotational states for the two Q_y exciton transitions. Dashed curves again represent calculations including nondegenerate interactions. As $|\boldsymbol{R}_b|$ is increased, the effects of non-degenerate interactions decrease approximately in parallel with the strength of the degenerate exciton interactions. The effects on the calculated dipole and rotational strengths are significant even when $|\boldsymbol{R}_b|$ is as large as 7 or 8 Å. (The strength of the CD bands measured experimentally is expected to decrease as $|\boldsymbol{R}_b|$ gets large, even

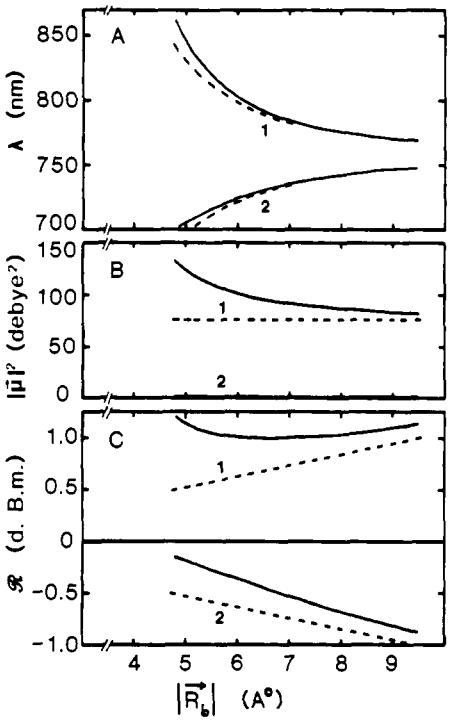

Fig. 7. Transition wavelengths (A), dipole strengths (B) and rotational strengths (C) calculated for transitions 1 and 2 of a BPh dimer, as a function of the center-to-center distance, $|\boldsymbol{R}_b|$. The orientation of $\boldsymbol{R}_b$ is fixed: $\boldsymbol{R}_b/|\boldsymbol{R}_b| =$ (0.099, 0.694, 0.714). Other structural parameters as in Fig. 3. Dashed and solid curves as in Fig. 4.

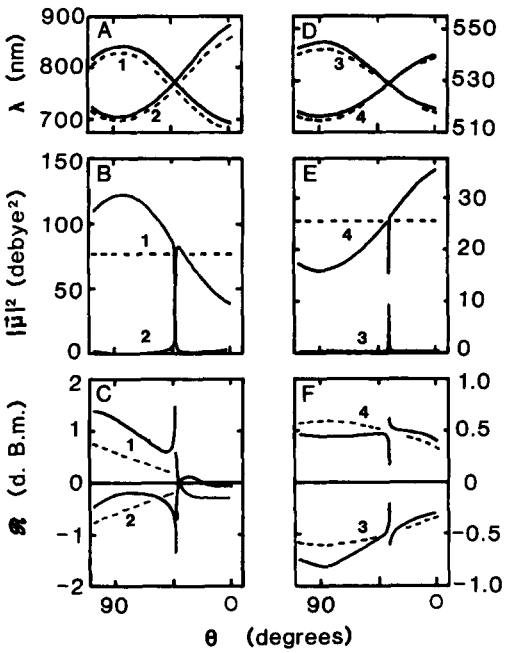

Fig. 8. Transition wavelengths, dipole strengths and rotational strengths for transitions 1–4 of a BPh dimer, as a function of the orientation of $\boldsymbol{R}_b$. The center-to-center distance $|\boldsymbol{R}_b|$ is fixed at 5.05 Å, and the z-component of $\boldsymbol{R}_b$ at 3.6 Å. $\boldsymbol{R}_b$ makes a constant angle of 45.52° with respect to the z-axis, and is rotated in a cone, as described in the text. θ is the azimuthal angle of rotation, with zero defined along the positive x-axis. Dashed and solid curves as in Fig. 4.

though the magnitudes of the rotational strengths continue to increase. The two exciton bands move closer together in energy, and their rotational strengths tend to cancel in the region of overlap.)

Fig. 8 shows how the spectroscopic properties depend on the direction of $\boldsymbol{R}_b$. The intermolecular distance $|\boldsymbol{R}_b|$ and the z-component of $\boldsymbol{R}_b$ are held constant at the values used for Fig. 3, and $\boldsymbol{R}_b$ is rotated in a cone about the z-axis. The position of the center of molecule b is described by the azimuthal angle $\theta = \arctan(r_y/r_x)$, where r_x and r_y are the x- and y-components of $\boldsymbol{R}_b$. The value $\theta = 90°$ thus means that molecule b is centered directly above the positive y-axis, $\boldsymbol{R}_b = (0, 3.54, 3.6)$ Å; $\theta = 180°$ means that it is centered above the negative x-axis, $\boldsymbol{R}_b = (-3.54, 0, 3.6)$ Å. Spectroscopic properties calculated for the Q_y and Q_x exciton transitions are shown. In order to obtain hyperchromism and a positive rotational strength for the main Q_y transision, molecule b must be displaced mainly along the y-axis ($\theta \approx 90°$ or 270°). Displacements along the x-axis ($\theta \approx 0°$ or 180°) give a larger Q_y exciton splitting (Fig. 8A), but give hypochromism and a weak negative rotational strength for this transition (Fig. 8B and C). The spectroscopic properties of the main Q_x transition have the opposite dependence on θ (Fig. 8D–F). The calculated rotational strengths are discontinuous at the points where the dimer's excited states are degenerate (θ near 42.5° and 37°), but the measured CD would be zero here.

Interactions of nondegenerate states also can affect the linear polarization of a dimer's transitions. The two exciton transition dipoles that result from a pair of degenerate molecular transitions must be orthogonal, but the mixing with additional, nondegenerate transitions generally removes this symmetry. With the structural parameters used for Fig. 3, the angle between the two Q_y transition dipoles, $\arccos(\boldsymbol{\mu}_1 \cdot \boldsymbol{\mu}_2/|\boldsymbol{\mu}_1||\boldsymbol{\mu}_2|)$, is calculated to be 77.2°. The angle between transitions 3 and 4 is 86.8°; that between transitions 5 and 6 is 89.8°; and that between transitions 7 and 8, 100.8°. Some of these angles change if molecule b is rotated 180° about its Q_x or Q_y transition dipole, but the effect is probably not large enough to be useful for determining structure.

Discussion

The calculations illustrated in Fig. 3 are reasonably successful in reproducing the main spectroscopic properties of BPh oligomers in lauryldimethylamine oxide. It seems clear that interactions between nondegenerate states are significant, and have to be considered in order to account for the spectra. Although the theory elaborated here is not sufficiently refined to determine the structure of the oligomers uniquely, the spectroscopic features require the neighboring molecules to be displaced by 3.5–4.0 Å in the y and z directions. The Q_y transition dipoles of the two molecules must be approximately but not exactly parallel or antiparallel ($\beta_y \approx 15°$ or 165°). The Q_x dipoles must be approximately side-by-side, but again not exactly parallel or antiparallel. These conclusions are consistent with the ideas that the dimer is stabilized by π–π interactions between the bacteriochlorin rings, and possibly by interactions of the C10a ester carbonyl group of one molecule with the C9 keto group of the other [5]. However, if the two molecules actually are this close together, orbital overlap and charge transfer between the molecules may contribute significantly to the optical properties of the dimer [26]. The theoretical approach used here could be extended by adding charge-transfer states to the set of excited states.

As noted above, the calculated rotational strengths are not entirely in accord with the observed CD spectrum. The main discrepancy is the presence of a negative CD band at 815 nm in the experimental spectrum [5]. In our view, it is unlikely that the 815 nm CD band represents the higher-energy Q_y exciton transition. This assignment would mean that the Q_y exciton interaction is relatively weak, which would be difficult to reconcile with the strong bathochromic shift and hyperchromism of the long-wavelength band, and with the nonconservative rotational strengths. The center of the higher- and lower-energy Q_y exciton bands would be at 832 nm, which is 74 nm to the red of the Q_y band of monomeric BPh (758 nm). This displacement would have to be attributed to effects other than exciton interaction. There is no evidence for specific chemical effects that could account for the spectral shift, because oligomers with similar absorption spectra can be obtained

with either BChl or PBh under a variety of conditions [5]. In addition, the positive CD maximum in the Q_y region coincides almost exactly with the maximum in the absorption spectrum [5]. If the exciton splitting were small, the positive and negative CD bands would overlap, and the observed positive maximum would be displaced to longer wavelengths. We therefore favor the view that the higher-energy Q_y transition is in the region of 700 nm, as indicated in Figs. 3, 4, 6 and 8, and that its dipole strength and rotational strength are both too weak for the transition to be seen experimentally.

If these arguments are correct, there remain several possible explanations for the discrepancies between the predicted and observed CD spectra. First, as emphasized above, the theory used here is limited by the neglect of orbital overlap, charge transfer, and permanent dipole moments, by the use of a point-dipole approximation rather than point-monopoles and by an oversimplified treatment of vibronic coupling. The 700–800 nm region of the spectrum could be influenced particularly strongly by vibronic coupling, because components of the monomeric Q_y transition that are not incorporated in the long-wavelength exciton band will contribute absorbance and CD in this region.

A second possibility is that the preparations of BPh oligomers that we have considered contain dimers with several different conformations, or contain a mixture of dimers, trimers and higher oligomers. The negative CD band at 815 nm could arise from a relatively small population of dimers that differ from the major species in, for example, the direction of displacement or the sense of rotation of molecule *b*. Such dimers would not necessarily contribute proportionally to the absorption spectrum, depending on their geometry.

Finally, the observed CD spectrum could be distorted by light scattering. Several authors have discussed the effects of light scattering on the measured CD of large particles [27–30]. It has been shown that the measured CD spectrum contains both absorptive (true CD) and dispersive (ORD) components [27]. The sign and magnitude of the ORD contribution depend on $d\sigma/d\eta$, where σ is the total optical cross-section of the particle for both absorption and scattering, and η is the real part of the particle's index of refraction. If $d\sigma/d\eta$ is negative, ORD could make a positive contribution to the rotational strength on the long-wavelength side of the main (850 nm) Q_y transition, and contribute a negative band on the short-wavelength side. this interpretation would be at odds with the observation that the postive CD maximum coincides with the abortion maximum. However, it does agree with the observation [5] that large aggregates of BPh in acetic acid-water mixtures, which are somewhat more scattering than the small aggregates formed in detergent micelles, have a stronger negative CD band near 800 nm and a second negative band near 865 nm, in addition to the positive band near 850 nm.

Many of the points made above should be relevant to the complexes of BChl, BPh and chlorophyll that occur in vivo. However, a thorough analysis of these complexes will have to consider the additional perturbations caused by interactions with the proteins. The nature of these interactions is still largely unknown.

Acknowledgements

We enjoyed particularly helpful discussions with Drs. M. Gouterman, R. Pearlstein, S. Boxer and A. Warshel. National Science Foundation Grant PCM 8016593 supported this work.

References

1 Sauer, K. (1978) Acc. Chem. Res. 11, 257–264
2 Drews, G. and Oelze, J. (1981) Adv. Microb. Physiol. 22, 1–92
3 Caplan, S. and Arntzen, C.J. (1982) in Photosynthesis. Energy Conversion by Plants and Bacteria (Govindjee, ed.), pp. 65–151, Academic Press, New York
4 Parson, W.W. (1982) Annu. Rev. Biophys. Bioenerg. 11, 57–80
5 Scherz, A. and Parson, W.W. (1984) Biochim. Biophys. Acta 766, 653–665
6 Gottstein, J. and Scheer, H. (1983) Proc. Natl. Acad. Sci. USA 80, 2231–2234
7 Tinoco, I., Jr. (1958) J. Am. Chem. Soc. 82, 4785–4790
8 Tinoco, I., Jr. (1962) Adv. Chem. Phys. 4, 113–157
9 Pearlstein, R. (1982) in Photosynthesis. Energy Conversion by Plants and Bacteria (Govindjee, ed.), pp. 295–330, Academic Press, New York
10 Zgierski, M.Z. and Pollikowski, M. (1982) Chem. Phys. Lett. 93, 613–616
11 Gouterman, M. (1961) J. Mol. Spectrosc. 6, 138–163
12 Weiss, C., Kobayashi, H. and Gouterman, M. (1965) J. Mol. Spectrosc. 16, 415–450

13 Weiss, C. (1972) J. Mol. Spectrosc. 44, 37–80
14 Petke, J.D., Maggiora, G.M., Shipman, L.L. and Christofferson, R.E. (1980) Photochem. Photobiol. 32, 399–414
15 Phillipson, K., Tsai, K. and Sauer, K. (1971) J. Phys. Chem. 75, 1140–1445
16 Johnson, W.C., Jr. and Tinoco, I., Jr. (1969) Biopolymers 8, 715–731
17 Carnahan, B., Luther, H.A. and Wilkes, J.O. (1969) Applied Numerical Methods, pp. 250–260, J. Wiley, New York
18 Hochstrasser, R.M. (1966) Molecular Aspects of Symmetry, Chs. 7 and 8, W.A. Benjamin, New York
19 Shipman, L. (1977) Photochem. Photobiol. 26, 287–292
20 Simpson, W.T. and Peterson, D.L. (1957) J. Chem. Phys. 26, 588–593
21 Hemenger, R.P. (1977) J. Chem. Phys. 66, 1795–1801
22 Hemenger, R.P. (1978) J. Chem. Phys. 68, 1722–1728
23 Friesner, R. and Silbey, R. (1981) Chem. Phys. Lett. 84, 365–369
24 Friesner, R. (1982) J. Chem. Phys. 76, 2129–2135
25 Pearlstein, R.M. and Hemenger, R.P. (1978) Proc. Natl. Acad. Sci. USA 75, 4920–4924
26 Warshel, A. (1979) J. Am. Chem. Soc. 101, 744–746
27 Schneider, A.S. (1971) Chem. Phys. Lett. 8, 604–608
28 Phillipson, K.D. and Sauer, K. (1973) Biochemistry 12, 3454–3458
29 Gregory, R.P.F. and Raps, S. (1974) Biochem. J. 142, 193–201
30 Bustamente, C., Tinoco, I., Jr. and Maestre, M. (1983) Proc. Natl. Acad. Sci. USA 80, 3568–3572